

ARTICLE OPEN



Ecological and societal effects of Central Asian streamflow variation over the past eight centuries

Feng Chen^{1,2}, Yujiang Yuan², Valerie Trouet³, Ulf Büntgen⁴, Jan Esper⁵, Fahu Chen^{6,7}, Shulong Yu², Miaogen Shen⁸, Ruibo Zhang², Huaming Shang², Youping Chen^{1,2} and Heli Zhang²

Understanding changes in water availability is critical for Central Asia; however, long streamflow reconstructions extending beyond the period of instrumental gauge measurements are largely missing. Here, we present a 785-year-long streamflow reconstruction from spruce tree rings from the Tien Shan Mountains. Although an absolute causal relationship can not be established, relatively high streamflow rates coincided roughly with the period of Mongol expansion from 1225 to 1260 CE and the rise of the Timurid Empire from 1361 to 1400 CE. Since overall wetter conditions were further found during the Zunghar Khanate period 1693–1705 CE, we argue that phases of streamflow surplus likely promoted oasis and grassland productivity, which was an important factor for the rise of inner Eurasian steppe empires. Moreover, we suggest that the streamflow variation might be critical for plague outbreaks in Central Asia, and propose several explanations for possible links with Europe's repeated Black Death pandemics. We demonstrate that 20th-century low streamflow is unprecedented in the past eight centuries and exacerbated the Aral Sea crisis, which is one of the most staggering ecological disasters of the twentieth century.

npj Climate and Atmospheric Science (2022)5:27; <https://doi.org/10.1038/s41612-022-00239-5>

INTRODUCTION

Climate is considered a key component in human evolution and history^{1–8}. Environmental conditions along the ancient Silk Road system contributed to the economic and cultural development in Eurasia since 1 CE^{6,9–21}. As the gateway from the Mongolian Plateau to Western Asia and Europe (Fig. 1), the Tien Shan Mountains and its surrounding oases played a critical role in nomadic migration into the inner Eurasian steppes^{22,23}. The Tien Shan Mountains not only supplied water and pastures for the steppe empires but also enabled trade caravans from East Asia to cross the vast Gobi Desert along the Silk Road system.

The hydroclimatic history of the Silk Road system over past centuries has been studied using tree-ring chronologies at high temporal resolution^{6,8,24–27}. Tree ring-based hydroclimatic reconstructions were also used to provide environmental insights into periods of historical transformation in Inner Asia, such as the invasion of the Huns in the 4–5th centuries, Turks in the 6–8th centuries and the Mongols in the first half of the 13th century^{6,13,19,21}. However, high-resolution streamflow reconstructions, as an important indicator of hydrological variation are still insufficient in Central Asia for interpreting the relationship between the supply of fresh water and historical societal changes in a long-term perspective. Here, we present an annually resolved streamflow reconstruction from the Tien Shan for the period 1225–2009 CE that covers the rapid expansion of the Mongolian Empire in the early 13th century. Our reconstruction is based on long-lived spruce trees from the different elevation area where tree growth is predominantly controlled by soil moisture availability.

RESULTS AND DISCUSSION

Streamflow reconstruction from the Tien Shan Mountains

The composite chronology was significantly positively correlated ($p < 0.05$) with temperature in the prior September and November and current February–March and June, August, September, and it was also significantly positively correlated ($p < 0.05$) with precipitation in the prior July and November and current July (Fig. 2a). Correlations were stronger with streamflow as well as with Normalized Difference Vegetation Index (NDVI) (Fig. 2a). Overall, correlations were strongest with July–April precipitation ($r = 0.64$, $p < 0.01$), August–April composite streamflow ($r = 0.77$, $p < 0.01$), November–October temperature ($r = 0.49$, $p < 0.01$) and August–October NDVI ($r = 0.72$, $p < 0.01$). Meanwhile, high correlation ($r = 0.69$, $p < 0.01$) between August–July composite streamflow and the composite chronology was also found. Warm temperatures with relatively abundant precipitation can prolong the growth period and lead to an increase in radial growth of spruce trees in high altitude area. We found that the seasonal response to the NDVI and streamflow tended to occur later than the responses to precipitation, suggesting that hydroclimate variability is the root cause of streamflow and vegetation change.

Based on the above analysis, to cover more months and develop a water-year composite streamflow reconstruction, we selected August–July composite streamflow as the target for our reconstruction. The model ($Y = 96.051 + 266.905X$) has significant skill based on the positive reduction of error (RE) and coefficient of efficiency (CE) statistics (Supplementary Table 3). The first differences of the tree-ring series with instrumental streamflow data were correlated with $r = 0.50$ ($p < 0.01$). The composite

¹Yunnan Key Laboratory of International Rivers and Transboundary Eco-Security, Institute of International Rivers and Eco-Security, Yunnan University, Kunming, China. ²Key Laboratory of Tree-ring Physical and Chemical Research of China Meteorological Administration/Xinjiang Laboratory of Tree-ring Ecology, Institute of Desert Meteorology, China Meteorological Administration, Urumqi, China. ³Laboratory of Tree-Ring Research, University of Arizona, Tucson, AZ, USA. ⁴Department of Geography, University of Cambridge, Cambridge, UK. ⁵Department of Geography, Johannes Gutenberg University, Mainz, Germany. ⁶Key Laboratory of Alpine Ecology, CAS Center for Excellence in Tibetan Plateau Earth Sciences and Institute of Tibetan Plateau Research, Chinese Academy of Sciences (CAS), Beijing, China. ⁷Key Laboratory of Western China's Environmental Systems (Ministry of Education), College of Earth and Environmental Sciences, Lanzhou University, Lanzhou, China. ⁸State Key Laboratory of Earth Surface Processes and Resource Ecology, Faculty of Geographical Science, Beijing Normal University, Beijing, China. ✉email: feng653@163.com; fhchen@itpcas.ac.cn

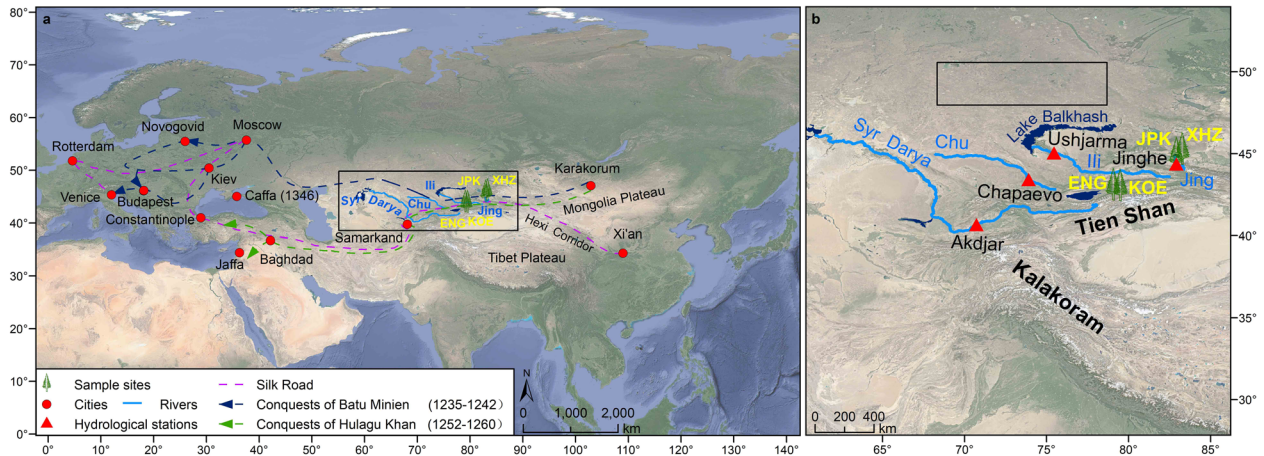


Fig. 1 Map of the study area. **a** Route of Mongol conquests (arrows), capital cities of the Mongolian Empire (Karakorum) and Timurid Empire (Samarkand), and silk road. The river basins are also shown (Rectangle). **b** Map showing the locations of the four sampling sites and hydrological stations with main rivers in Central Asia. The Pre-Balkhash plague focus area of southern Kazakhstan is also shown (Rectangle).

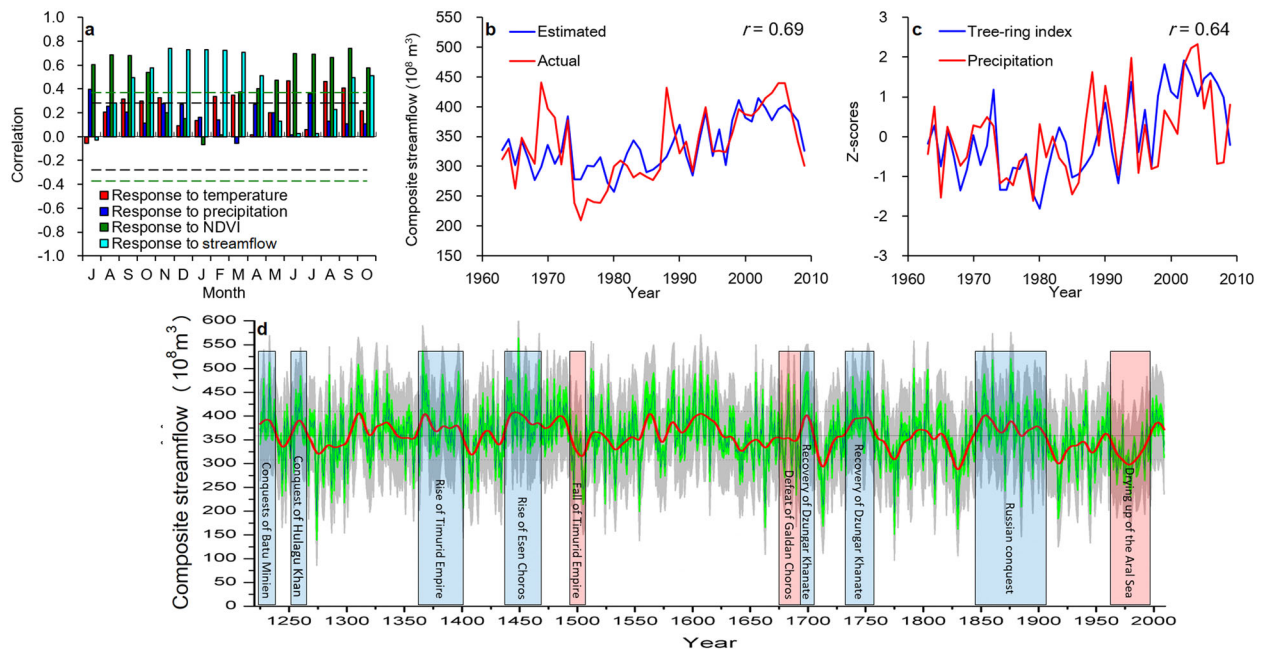


Fig. 2 Response of tree-ring width to climate, NDVI and streamflow and streamflow reconstruction. **a** Responses of the composite chronology to monthly mean temperatures, precipitation sum, composite streamflow, and NDVI. Correlations are computed from the previous year in July to the current year in September over the common period. The horizontal dashed lines indicate the 95% significance levels. **b** Actual and estimated total streamflow of the previous August to the current July for 1962–2009. **c** Comparison between tree-ring index and total July–April precipitation for 1962–2009. **d** Reconstructed August–July composite streamflow of the Syr Darya, Ili, Chu, and Jing rivers (blue curve) shown together with the two-tailed 95% bootstrap confidence limits (green) and ± 1 root mean square error (RMSE) uncertainty estimates (gray) since 1225 CE. Red curve is a 21-year low pass filter. Reconstructed streamflow from 1225 to 1239, 1252 to 1260, 1361 to 1400, 1437 to 1467, 1494 to 1511, 1678 to 1692, 1693 to 1705/1731 to 1756, 1844 to 1905 and 1961 to 1996, corresponding to conquests of Batu Minien, Hulagu Khan's conquests, rise of Timurid Empire, rise of Esen Choros, fall of Timurid Empire, defeat of Galdan Choros, recovery of Dzungar Khanate, Russian conquest and drying up of the Aral Sea, respectively. Blue and red boxes represent high and low streamflow conditions, respectively. Central horizontal line shows the average of streamflow estimates, and dotted lines indicate one standard deviation.

chronology showed good consistency with the regional streamflow and precipitation variations (Fig. 2b, c). We also found strong positive correlations up to $r = 0.72$ ($p < 0.01$; 1981–2009) with the August–October NDVI, and some significant positive correlations were found in the Central and Eastern European plains as well as in Scandinavia. Moreover, significant negative correlations were also found in the Mediterranean Basin, Middle East, and western Asia (Fig. 3a). The PDSI reconstruction of the Mediterranean Basin¹⁶ also had a good correlation with NDVI, and the spatial

distribution pattern was different from that of our streamflow reconstruction (Fig. 3b and Supplementary Fig. 4).

The average annual (August–July) reconstructed streamflow (1225–2009 CE) was $358.9 \times 10^8 \text{ m}^3$, with a standard deviation of $51.1 \times 10^8 \text{ m}^3$. The streamflow reconstruction is the longest streamflow reconstruction current in Central Asia, and covers the two Mongol expansions in 1235–1242 CE and 1252–1260 CE^{9,14,28,29}, the onset and establishment of the Black Death in 1346–1348 CE (Supplementary Table 2)¹⁵, the rise of the Timurid

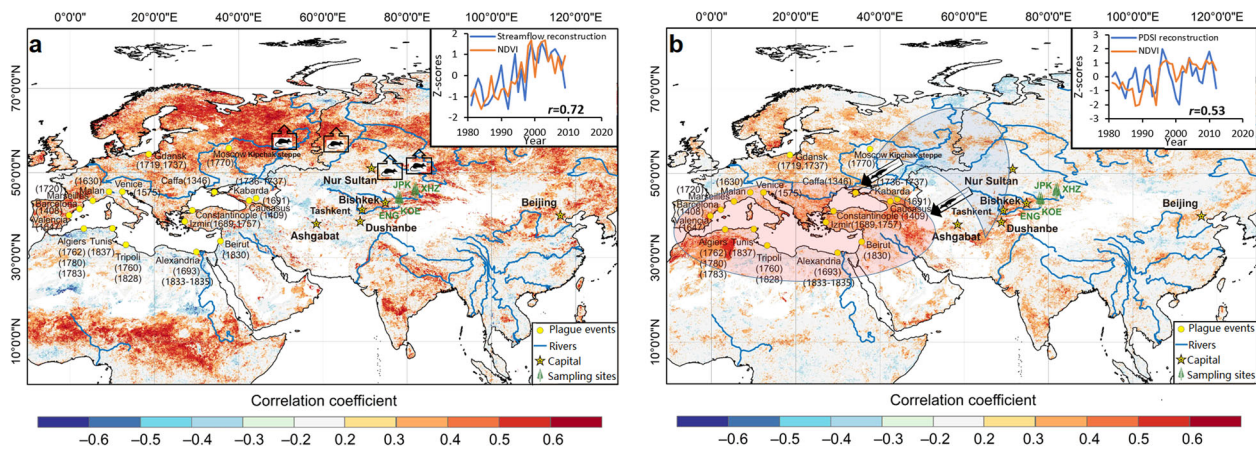


Fig. 3 Spatial correlations between the dendrohydrological reconstructions and the gridded NDVI dataset⁶². **a** Correlation patterns of the streamflow reconstruction with August-October NDVI, a satellite-derived measure of grassland productivity, over their period of overlap (1981–2009). Insignificant correlations ($P > 0.05$) are masked out. The mouse icons indicate that the rodent population density increased under the good vegetation and water conditions in Central Asia. The inset figure shows the comparison between regional NDVI (averaged over 39–45°N, 77.5–86.5°E) and reconstructed streamflow (this study). **b** Correlation patterns of the PDSI reconstruction of the Mediterranean Basin with July–September NDVI. The mouse icons and arrows show that poor vegetation conditions in Central Asian steppe (blue shape) forced the rodent to migrate to the Mediterranean basin and Western Asia (red circle) with the good vegetation and water conditions. The inset figure shows the comparison between regional NDVI (averaged over 30–45°N, –5–37°E) and reconstructed PDSI¹⁶. The numbers in parentheses in the maps indicating the recorded time of plague outbreaks per city.

Table 1. Some high and low periods in the streamflow reconstruction of Tien Shan Mountains and comparisons with important historical events.

Historical events	Response period	NDVI	Mean ($1 \times 10^8 \text{ m}^3$)	Percentage ($> \text{Mean}$)	Percentage ($> \text{Mean} + \sigma$)	Percentage ($< \text{Mean}$)	Percentage ($< \text{Mean} - \sigma$)
	1225–2009	0.1835	358.9	51.3%	15.5%	48.7%	15.9%
Conquests of Batu Minien	1225–1239	0.1910 (4%)	388.6	93.3%	20.0%		
Hulagu Khan's conquest	1252–1260	0.1913 (4%)	389.5	88.9%	33.3%		
Rise of Timurid Empire	1361–1400	0.1893 (3%)	381.8	65.0%	27.5%		
Rise of Esen Choros	1437–1467	0.1939 (5%)	399.8	77.4%	48.4%		
Fall of Timurid Empir	1494–1511	0.1753 (–5%)	326.8			77.8%	33.3%
Defeat of Galdan Choros	1678–1692	0.1797 (–2%)	344.1			66.7%	26.7%
Recovery of Dzungar Khanate	1693–1705	0.1919 (4%)	391.9	76.9%	30.8%		
	1731–1759	0.1899 (3%)	384.1	79.3%	24.1%		
Russian conquest	1844–1905	0.1879 (2%)	376.3	69.4%	16.1%		
Drying up of the Aral Sea	1961–1996	0.1734 (–6%)	319.0			86.1%	44.4%

Empire in 1361–1400 CE, the rise and fall of the Zunghar Khanate in 1678–1756 CE^{29,30}, and the recent drying up of the Aral Sea from the 1960s to present³¹ (Table 1).

Streamflow levels were mainly above average from 1225 to 1260 CE during the westward conquests of the Mongols⁹, including pluvials from 1225 to 1239 CE during the conquests of Batu Minien, and from 1252 to 1260 CE during Hulagu Khan's conquest. These pluvial periods were interrupted by a brief period of low streamflow (1240–1251 CE) followed by a multidecadal dry period in the late 13th century.

Another pluvial occurred in the second half of the 14th century during the rise of the Timurid Empire (1361–1400 CE), when streamflow was above average from 1364 to 1371, 1381 to 1387, and 1394 to 1400 CE. The decline of the Timurid Empire in 1507 CE, on the other hand, fell within an 18-year period of low streamflow conditions (1494–1511 CE).

During a pluvial from 1437 to 1467 CE, the king of the Oirat Mongols, Esen Choros, reunited the Mongolian tribes and captured the Zhengtong emperor of the Ming Empire after the

Battle of Tumu in 1449 CE⁹. This series of events allowed the Oirat Mongols to control the Tien Shan from the mid-15th century until the attack of the Qing Empire (1755–1757 CE)³⁰ and found the Dzungar Khanate in 1634 CE. The army of Galdan Choros, a descendant of Esen Choros, was defeated by the Qing Empire during a relatively low streamflow period in 1678–1692 CE, although the power of the Dzungar Khanate was restored during two subsequent high-streamflow periods in 1693–1705 and 1731–1759 CE. This latter period was characterized by frequent wars with the Eastern Mongols, Kazak Khanate, and Qing Empire. In the warm-wet climatic condition³², epidemics resulted from wars were expanded in the Dzungar Khanate, and 40% of the Dzungar Khanate population died of smallpox³³. Due to the prevalence of smallpox and the civil strife in the Dzungar Khanate, the Qing Empire conquered the Dzungar Khanate³⁰, and the subsequent low streamflows from 1758 to 1790 CE coincided with weak hostile forces in Xinjiang.

In the late 19th century (1844–1905 CE), the period during which Russia gradually completed its conquest of Central Asia³⁴,

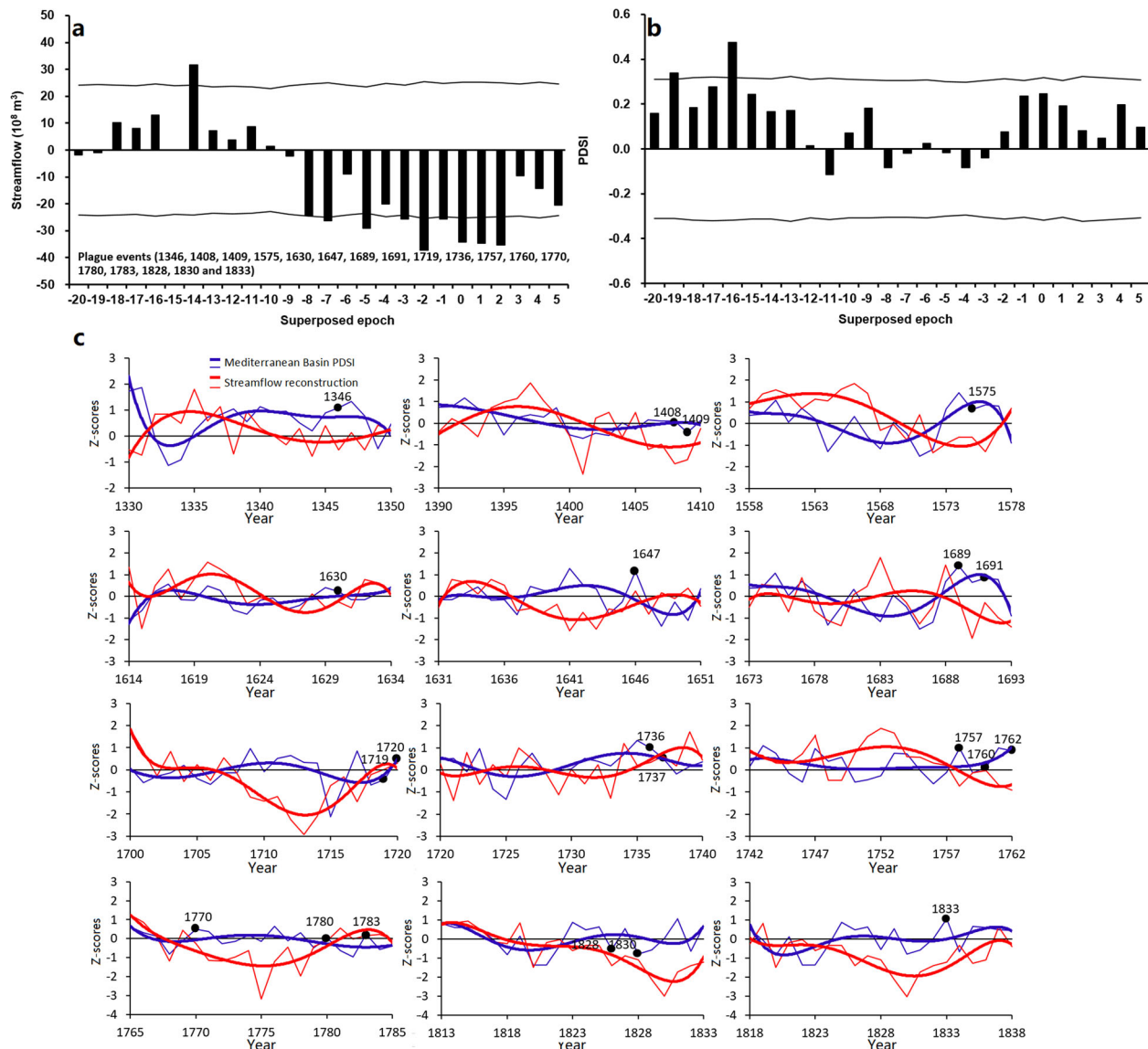


Fig. 4 The response of Central Asian streamflow to the plague outbreaks. Results of the superposed epoch analysis (SEA) testing the response of Central Asian streamflow (a) and PDSI of the Mediterranean Basin (b) to the outbreak of the plague events (Supplementary Table 2). The solid lines indicate the 95% significance level. **c** Comparison between the reconstructed August–July total streamflow (red curve) and PDSI reconstruction of the Mediterranean Basin (blue curve)¹⁶. Thick curves are trend lines of the reconstructions along with the circulars representing the outbreak years of the plague in the Mediterranean Basin and Europe.

the streamflow was generally above average. The mean streamflow value ($332.0 \times 10^8 \text{ m}^3$) during the 20th century (1900–1999 CE) was lower than in any other century since 1225 CE (Supplementary Table 4). The low streamflow (−6%) during the period 1961–1996 contributed to the continuous reduction in upstream water supplies and marked the unprecedented drying of the Aral Sea and its surroundings³¹.

We find significantly high streamflows 15 years prior to the 18 plague events of Europe and the Mediterranean Basin that linked with Asian plague outbreak (Supplementary Table 2). After these abnormal streamflow increases, the long-term downward trends of streamflow or some drought events occurred until the outbreak of the plague in Europe and the Mediterranean Basin, and the drying process may be last for up to a decade, and on the contrary, the Mediterranean Basin and Near East is in the relatively humid state when the plagues occurred (Fig. 4). Results from GCA

also support the claim that streamflow Granger-cause plague outbreaks ($P < 0.05$) (Supplementary Table 5).

Impact of river streamflow on the rise and fall of Central Asian empires

The Mongol Empire, the Timurid Empire, the Oirat Mongols, and the Dzungar Khanate had some important influences on the history of Eurasia, such as the Mongol conquests^{9,28,29}, the Timur conquests^{29,35}, the Turko-Mongol fusion³⁵, the Mongolia unification by Esen Choros, the battle of Tumu³⁶ and the Dzungar–Qing Wars^{30,37,38}. Such outstanding military and political accomplishments likely required a strong material base that relied on grassland and oasis productivity, favorable climatic conditions, and abundant water. Because rainfall in Central Asia is scarce, the rivers originating from Tien Shan glaciers became the most valuable water resource, greatly affecting oasis agriculture and

grassland animal husbandry, as well as the power balance among different empires in Central Asia^{39,40}. In contrast to oasis settlers, ancient nomadic tribes mainly depended on grazing, hunting, and gathering for food⁴¹. Moreover, the survival and reproduction of livestock and wild animals are closely linked to the net primary productivity (NPP) of the steppe⁶, which in turn depends on rainfall and water⁴². As a good indicator of NPP, the significant positive correlation of NDVI data with our streamflow reconstruction for the Central Asian steppe supports this connection. The high streamflow periods of 1225–1239, 1252–1260, 1361–1400, 1437–1467, 1693–1705, and 1731–1759 CE were likely associated with humid conditions and relatively high NDVI values (+4.1%) (Fig. 2d); therefore, the grassland provided more food for the armies of Central Asian empires (Table 1). During that time, more water drained from the Tien Shan into the arid plains, lakes, and wetlands, including the Aral Sea, Balkhash lake, and Ebinur lake. This increased water might have led to rising NPP in the middle and lower reaches of nearby rivers, which was conducive to the armies of Central Asian empires advancing westward towards Europe and Western Asia. Adequate water resources also promoted the restoration and development of oasis agriculture, and the armies had access to pasture and food supplies from the conquered oases. The most typical examples are Samarkand and Ili. As the capital of the Timurid Empire, oasis city Samarkand grew to have a population of about 150,000 during the second half of the 14th century, and a large number of artists, craftsmen, and scholars gathered from all over the country. By forced Uighurs to move to Ili and other parts of Dzungaria to engage in agricultural activities on farms, the Dzungar Khanate established a progressive oasis agriculture in Ili and its surrounding regions^{38,43}. The transfer of the political center of the Dzungar Khanate to Ili supports the hypothesis of abundant wealth from highly productive farms and steppes supporting the concentrations of nomadic and semi-nomadic tribes. Access to water enabled the Timurid Empire and Dzungar Khanate leadership to establish military and political power. Of particular interest is the similar response of NDVI of Central Asia and the Central and Eastern European plains to our streamflow reconstruction (Fig. 3a), which may be linked to the middle-latitude westerly circulations, with contributions from middle and high latitudes^{44–47}. Wet conditions in the Central and Eastern European plains also supplied more fodder and clean water for the Mongol invasions in the early-mid-13th century.

Prolonged bad climate conditions and the resulting poor economies also drove the outward expansion of Central Asian invaders, leading to events such as the fall of the Timurid Empire and the rise of the Mughal Empire^{13,19,48}. Although the Timurid Empire was destroyed during the low-streamflow phase of 1494–1511 CE with a relatively low NDVI (–5%), the influence of the empire did not completely disappear. The remnants of the Timurid Empire entered the Indian subcontinent with the relatively good climate and good economic conditions in 1510s^{48,49}, and established the Mughal Empire in India.

Although some scientists consider climate change to have been an important driver of the rise of the Mongol Empire and the migration of nomadic tribes in Eurasia^{6,14}, the role of river streamflow in arid to semiarid Central Asia during the rise of the empire has not been addressed. Our streamflow reconstruction suggests that the rise of the Central Asian empires during the last 750+ years was related to favorable water conditions, which were conducive to increased pasture yields and powerful nomadic tribes. Perhaps even more importantly, sufficient water resources met the need for oasis irrigation and provided resources for the rise of the empire and the foundation of a persistent civilization. The large-scale expansions and conquests based on sufficient water resources not only enabled the empires to obtain greater territories and resources but also eventually affected Eurasian civilizations. At the same time, it needs to be emphasized that the rise and fall of the Central Asian empires did not depend entirely

on the hydroclimate-driven NDVI change, which simply provided a substantial material base. Although hydroclimate changes are the far-reaching process affecting human society, the rise and fall of empires are also influenced by military power, the political system, the ability of leaders, and other factors, especially in multi-ethnic and multicultural Central Asia^{9,29,35}.

Role of river streamflow in the spread of plague

The correlation between the streamflow estimates and NDVI values indicates that the grassland productivity in mountainous terrain benefits from abundant water, providing favourable conditions for the pastures and livestock of nomadic tribes. However, increased precipitation that leads to high streamflow also supports rodents in grasslands and mountains, thus leading to an increased risk of plague^{10,50–53}. We detected significantly high streamflows 15 years prior to the 18 plague events of Europe and the Mediterranean Basin that were linked with previous plague outbreaks in Asia (Fig. 4a and Supplementary Table 2). This phenomenon resembles other finding in surrounding area¹⁵, and suggests the influence of solar activity and its related atmospheric circulations on the hydroclimate variation^{54,55} (Supplementary Fig. 5). The high streamflow period of 1332–1337 CE preceded the onset and establishment of Europe's Black Death from 1346 to 1348 CE by approximately a decade. More seriously, with the low streamflows, drought events, and decrease in the NDVI (–2.9%) before the outbreak of the plague, significant decreases in the amount of food available to rodents were observed (Fig. 3). This change would have led to changes in the population structure of rodents in Central Asia and caused rodent migration⁵¹. Meanwhile, some studies have shown that the Mediterranean Basin, the Near East, and Western Asia were relatively humid during the Black Death periods^{12,16}, which may have provided rodents with sufficient food thereby increasing the risk of plague outbreak. The NDVI and precipitation patterns also support such a connection (Fig. 3 and Supplementary Fig. 4). As shown in Figs. 3 and 4a, the abnormal decrease in the NDVI persisted for 5–10 more years before the outbreak of plague not only occurred in the Tien Shan and surrounding grasslands but also may have existed in the Kipchak steppe stretching from the northern shores of the Black Sea as far east as the Aral Sea and Caspian Sea. After the unification of Inner Asia by the Mongol Empire, the trade routes of the northern steppe began to prosper. With the increase in logistics and human movement, the risk of plague transmission in the Mediterranean Basin, the Middle East, and Western Asia was further increased. The most typical example was observed in 1346 CE. When the Golden Horde army attacked the trading city Caffa at the Black Sea coast⁵⁶, it also brought plague from the natural foci north and east of the Caspian Sea and Black Sea in the upper reaches of the rivers (with low NDVI) to the Mediterranean Basin and Near East (with relatively high NDVI) (Fig. 4 and Supplementary Fig. 4). Therefore, the spread of plague may not have been simply caused by the hydroclimate-driven NDVI change and its associated rodent migration but also by anthropogenic activities, such as trade activities or military activities. Nevertheless, large-scale comparisons between tree-ring records still provide evidence of the possible role of hydroclimate variation in the outbreak of plague.

Link between 20th century low streamflows and the Aral Sea crisis

The 785-year streamflow reconstruction presented here provides a long-term perspective for the recent period of rapid economic, social and cultural transformation in Central Asia. During the 20th century (with the unprecedented warming), regional water resources were less abundant than during any other period of the past seven centuries, including the ten decades when they were below the long-term average. Based on the range of

streamflows reconstructed from 1901 to 1999, there would be a 70% chance that streamflow would not meet or exceed $358.9 \times 10^8 \text{ m}^3$. Thus, in almost seven out of every 10 years the surface water supply would not be sufficient to meet the water right allocations and river flow targets. The persistent low runoff in Tien Shan with climate warming also raises doubts over the sustained water resources supply to meet the rapidly growing water consumption in Central Asia, and this is a vital information that can not be obtained from short instrumental records. Even worse, these conditions also occurred during a period of rapid and widespread agricultural development in the former Soviet Republics of Central Asia. After World War II, the former Soviet Union built reservoirs and canals and developed large regions of Central Asia into granary and cotton production bases, including Uzbekistan, which is still the second-largest cotton exporter in the world^{57,58}. The combination of continuous natural streamflow reduction (−6%) and dramatically increased water irrigation successively reduced river streamflow into many lakes of Central Asia⁵⁹, and Aral Sea has lost 90% of its volume over the past 50 years and caused Central Asia's largest ecological disaster³¹. Thus, although the Aral Sea crisis is mainly due to unreasonable water diversion, our tree-ring-based reconstruction implying that unprecedented 20th century low streamflow has exacerbated the crisis, and this valuable paleo-hydrologic information is in the process of being incorporated into reasonable water resources management policy for Central Asia.

Based on tree-ring data from the Tien Shan, China, and Kyrgyzstan, we presented a streamflow reconstruction for the Tien Shan that revealed Central Asian streamflow variation over the past 785 years. The atypical hydrological conditions of the Tien Shan, such as those occurring during 1361–1400 CE and the 20th century, had far-reaching consequences, including the rise of empires, civilization formation, and ecological changes in Central Asia. The pluvial periods in our 785-year composite streamflow reconstruction associated with the rise of Central Asian steppe empires, and plague spread were marked by sequential years (≥ 4 years) of above/below average streamflow rather than individual years of extremes. Although water resources played an important role in the historical and societal changes of Central Asia, it must be emphasized that water resources represent only one of the factors that influenced these complex historical processes. Due to the warm-wet climate in Central Asia, streamflow has also shown significant recovery since 1987⁶⁰. Due to the accelerated melting of glaciers in the warming 21st century, the rivers originating in the Tien Shan will benefit from additional meltwaters within a relatively short time³⁹. However, in the future, as temperatures continue to rise and glaciers disappear, evaporation will exceed precipitation; as a result, ecological disasters similar to the disappearance of the Aral Sea will likely increase/continue in Central Asia. Therefore, it is necessary for Central Asian countries to establish a rational water distribution mechanism to ensure sustainable development and maintain ecological balance.

METHODS

Streamflow and climate data

The study focused on the Tien Shan, China, and Kyrgyzstan, the wettest region in Central Asia. Tien Shan, referred to as Central Asian water tower, are the source of some of Central Asian major rivers, include Syr-Darya and Ili river, and also help to regulate regional climate^{31,39} (Fig. 1). As the most densely populated area in Central Asia, this region is an important part of the Silk Road in Central Asia and the meeting point of eastern and western civilizations⁹. Many imperial capitals were built in the study area, include the Timurid Empire (Samarkand) and the Dzungar Khanate (Ili), and developed splendid civilizations. The glacier retreats in Tien Shan with climate warming raises doubts over the sustained fresh water supply to meet the rapidly growing water consumption³⁹. At the same time, the conflict over water resources in the region has become increasingly acute,

and the irrational use of water resources of transboundary rivers caused the Aral Sea crisis^{31,59}. Monthly streamflow data are obtained from five downstream hydrologic hydrometric stations, include Akdjar, Ushjarma, Chapaeva, and Jinghe for the period 1962–2009 (Supplementary Table 1 and Supplementary Fig. 1). The streamflow data were used to produce time series of monthly composite streamflow and correlation analysis was used to evaluate relationships to the tree-ring chronology. We also used Climatic Research Unit (CRU) gridded monthly climate data (averaged over 77.5–86.5°N, 39–45°E, 1962–2009)⁶¹ and Normalized Difference Vegetation Index (NDVI, averaged over 77.5–86.5°N, 39–45°E, 1981–2009)⁶² data to better understand the climatic controls on the vegetation growth.

Tree-ring data and streamflow reconstruction trials

The composite chronology is based on raw measurements of tree-ring widths derived from 396 individual series from 210 drought-sensitive spruce trees that were growing at four sampling sites between 42–45°N and 79–84°E (Supplementary Table 1 and Supplementary Fig. 2). The RBAR (mean correlation between ring-width series) and expressed population signal (EPS) used 50-year windows with a lag of 25 years to evaluate the adequacy of replication in the early years of the chronology⁶³ (Supplementary Fig. 3). We truncated the composite chronology at the year 1225 CE based on the EPS value of 0.85, when sample depth dropped below six series from three trees. A simple linear regression model was used to develop a composite streamflow reconstruction for the Tien Shan, and model skill was verified with standard methods⁶⁴. In order to indicate the response of the NDVI patterns in Eurasia to the regional reconstructions, we also used the KNMI Climate Explorer⁶⁵ to calculate spatial correlation maps of our streamflow reconstruction and the PDSI reconstruction for the Mediterranean Basin¹⁶ with the NDVI dataset. We investigated hydrology-driven plague outbreak signals in the Tien Shan streamflow reconstruction using a Superposed Epoch Analysis (SEA, <https://rdrr.io/cran/dplr/man/sea.html>)⁶⁶ and Granger Causality Analysis (GCA)⁶⁷. Details on the research area, data, methods, and analyses are provided in the supporting information.

DATA AVAILABILITY

The streamflow reconstruction in this study is available in a data file published along with this article. The streamflow reconstruction is also downloaded from the Mendeley Data Repository Center (<https://doi.org/10.17632/bwbpbjmnhb.1>). The data that support the plots and other findings of this study are available from the corresponding authors upon request.

CODE AVAILABILITY

The code to carry out the current analyses is available from the corresponding authors upon request.

Received: 6 April 2021; Accepted: 9 February 2022;
Published online: 30 March 2022

REFERENCES

- deMenocal, P. B. Cultural responses to climate change during the Late Holocene. *Science* **292**, 667–673 (2001).
- Kuper, R. & Kröppel, S. Climate-controlled Holocene occupation in the Sahara: motor of Africa's evolution. *Science* **313**, 803–807 (2006).
- Cook, E. R. et al. Asian monsoon failure and megadrought during the last millennium. *Science* **328**, 486–489 (2010).
- Buckley, B. M. et al. Climate as a contributing factor in the demise of Angkor, Cambodia. *Proc. Natl Acad. Sci. USA* **107**, 6748–6752 (2010).
- Aimers, J. & Hodell, D. Societal collapse: Drought and the Maya. *Nature* **479**, 44–45 (2011).
- Pederson, N. et al. Pluvials, droughts, the Mongol Empire, and modern Mongolia. *Proc. Natl Acad. Sci. USA* **111**, 4375–4379 (2014).
- Kathayat, G. et al. The Indian monsoon variability and civilization changes in the Indian subcontinent. *Sci. Adv.* **3**, e1701296 (2017).
- Hessl, A. et al. Past and future drought in Mongolia. *Sci. Adv.* **4**, e1701832 (2018).
- Grousset, R. *The empire of the steppes: a history of Central Asia* (Rutgers University Press, 1970).
- Stenseth, N. C. et al. Plague dynamics are driven by climate variation. *Proc. Natl Acad. Sci. USA* **103**, 13110–13115 (2006).

11. Beckwith, C. I. *Empires of the Silk Road: A History of Central Eurasia from the Bronze Age to the Present* (Princeton University Press, 2009).
12. Büntgen, U. et al. 2500 years of European climate variability and human susceptibility. *Science* **331**, 578–582 (2011).
13. Büntgen, U. et al. Cooling and societal change during the Late Antique Little Ice Age from 536 to around 660 AD. *Nat. Geosci.* **9**, 231–236 (2016).
14. Büntgen, U. & Di Cosmo, N. Climatic and environmental aspects of the Mongol withdrawal from Hungary in 1242 CE. *Sci. Rep.* **6**, 25606 (2016).
15. Schmid, B. V. et al. Climate-driven introduction of the Black Death and successive plague reintroductions into Europe. *Proc. Natl Acad. Sci. USA* **112**, 3020–3025 (2015).
16. Cook, E. R. et al. Old World megadroughts and pluvials during the Common Era. *Sci. Adv.* **1**, e1500561 (2015).
17. Cook, B. I., Anchukaitis, K. J., Touchan, R., Meko, D. M. & Cook, E. R. Spatiotemporal drought variability in the Mediterranean over the last 900 years. *J. Geophys. Res.: Atmos.* **121**, 2060–2074 (2016).
18. Ljungqvist, F. C. Northern Hemisphere hydroclimate variability over the past twelve centuries. *Nature* **532**, 94–98 (2016).
19. Di Cosmo, N., Oppenheimer, C. & Büntgen, U. Interplay of environmental and socio-political factors in the downfall of the Eastern Türk Empire in 630 CE. *Clim. Change* **145**, 383–395 (2017).
20. Moffa-Sánchez, P. & Hall, I. R. North Atlantic variability and its links to European climate over the last 3000 years. *Nat. Comm.* **8**, 1726 (2017).
21. Guedes, J. D. A. & Bocinsky, R. K. Climate change stimulated agricultural innovation and exchange across Asia. *Sci. Adv.* **4**, eaar4491 (2018).
22. Pritchard, H. D. Asia's glaciers are a regionally important buffer against drought. *Nature* **545**, 169–174 (2017).
23. Frachetti, M. D., Smith, C. E., Traub, C. M. & Williams, T. Nomadic ecology shaped the highland geography of Asia's Silk Roads. *Nature* **543**, 193–198 (2017).
24. Yuan, Y. et al. The potential to reconstruct Manasi River streamflow in the northern Tien Shan Mountains (NW China). *Tree-ring Res.* **63**, 81–94 (2007).
25. Liu, Y. et al. Tree-ring hydrologic reconstructions for the Heihe River watershed, western China since AD 1430. *Water Res.* **44**, 2781–2792 (2010).
26. Gou, X. et al. Tree-ring based streamflow reconstruction for the Upper Yellow River over the past 1234 years. *Chin. Sci. Bull.* **55**, 4179–4186 (2010).
27. Yang, B., Qin, C., Shi, F. & Sonechkin, D. M. Tree ring-based annual streamflow reconstruction for the Heihe River in arid northwestern China from AD 575 and its implications for water resource management. *Holocene* **22**, 773–784 (2012).
28. Di Cosmo, N. State formation and periodization in Inner Asian history. *J. World Hist.* **10**, 1–40 (1999).
29. Christian, D. *A History of Russia, Central Asia, and Mongolia, Volume II: Inner Eurasia from the Mongol Empire to Today, 1260-2000* (Wiley-Blackwell, 2018).
30. Perdue, P. C. *China Marches West: The Qing Conquest of Central Eurasia* (Harvard University Press, 2005).
31. Micklin, P. P. Desiccation of the Aral Sea: A water management disaster in the Soviet Union. *Science* **241**, 1170–1176 (1988).
32. Yu, S., Yuan, Y., He, Q., Li, J. & Wu, Z. J. Reconstruction of temperature series from A.D. 1468 to 2001 in the Jinghe, Xinjiang. *J. Glaciol. Geocryol.* **29**, 374–379 (2007).
33. Wei, Y. *Sheng wu ji (圣武记) (A Record of the Qing Dynasty's Military Campaigns)* (Zhonghua Shu Ju, 1984).
34. Saray, M. The Russian conquest of Central Asia. *Cent. Asian Sur.* **1**, 1–30 (1982).
35. Chaliand, G. & Berrett, A. M. *Nomadic empires: from Mongolia to the Danube* (Routledge, 2017).
36. Feng, L. Tumu crisis and the weakness of the military system of Ming dynasty. *Asian Soc. Sci.* **5**, 12–18 (2009).
37. Wright, D. C. Gong Zizhen and His Essay on the "Western Regions. *Asian Stud.* **46**, 761–790 (1987).
38. Brophy, D. *Uyghur Nation* (Harvard University Press, 2016).
39. Sorg, A., Bolch, T., Stoffel, M., Solomina, O. & Beniston, M. Climate change impacts on glaciers and runoff in Tien Shan (Central Asia). *Nat. Clim. Change* **2**, 725–735 (2012).
40. Toonen, W. H. et al. A hydromorphic reevaluation of the forgotten river civilizations of Central Asia. *Proc. Natl Acad. Sci. USA* **117**, 32982–32988 (2020).
41. Sinor, D. & Dénes, S. (eds). *The Cambridge History of Early Inner Asia* Vol. 1 (Cambridge University Press, 1990).
42. Nemani, R. R. et al. Climate-driven increases in global terrestrial net primary production from 1982 to 1999. *Science* **300**, 1560–1563 (2003).
43. Dani, A. H. & Masson, V. M. *History of Civilizations of Central Asia* (UNESCO Publishing, 2003).
44. Rogers, J. C. & Van Loon, H. The seesaw in winter temperatures between Greenland and northern Europe. Part II: Some oceanic and atmospheric effects in middle and high latitudes. *Monthly Weather Rev.* **107**, 509–519 (1979).
45. Hurrell, J. W. Decadal trends in the North Atlantic Oscillation: regional temperatures and precipitation. *Science* **269**, 676–679 (1995).
46. Aizen, E. M., Aizen, V. B., Melack, J. M., Nakamura, T. & Ohta, T. Precipitation and atmospheric circulation patterns at mid-latitudes of Asia. *Int. J. Climatol.* **21**, 535–556 (2001).
47. Chen, F. H., Huang, W., Jin, L., Chen, J. & Wang, J. Spatiotemporal precipitation variations in the arid Central Asia in the context of global warming. *Sci. China Earth Sci.* **54**, 1812–1821 (2011).
48. Yadava, A. K., Braeuning, A., Singh, J. & Yadav, R. R. Boreal spring precipitation variability in the cold arid western Himalaya during the last millennium, regional linkages, and socio-economic implications. *Quat. Sci. Rev.* **144**, 28–43 (2016).
49. Dowson, J. *The History of India as Told by its Own Historians—The Muhammadan Period* (Edited from the Posthumous Papers of the Late Sir H.M. Eliot) Vol. 1. (Trubner and Company, 1867).
50. Dickman, C. R., Mahon, P. S., Masters, P. & Gibson, D. F. Long-term dynamics of rodent populations in arid Australia: The influence of rainfall. *Wildl. Res.* **26**, 389–403 (1999).
51. Linné Kausrud, K. et al. Climatically driven synchrony of gerbil populations allows large-scale plague outbreaks. *P. Roy. Soc. B: Biol. Sci.* **274**, 1963–1969 (2007).
52. Samia, N. I. et al. Dynamics of the plague–wildlife–human system in Central Asia are controlled by two epidemiological thresholds. *Proc. Natl Acad. Sci. USA* **108**, 14527–14532 (2011).
53. Xu, L. et al. Nonlinear effect of climate on plague during the third pandemic in China. *Proc. Natl Acad. Sci. USA* **108**, 10214–10219 (2011).
54. Ogi, M., Yamazaki, K. & Tachibana, Y. Solar cycle modulation of the seasonal linkage of the North Atlantic Oscillation (NAO). *Geophys. Res. Lett.* **30**, 2170 (2003).
55. Gray, L. J., Woollings, T. J., Andrews, M. & Knight, J. Eleven-year solar cycle signal in the NAO and Atlantic/European blocking. *Quar. J. Roy. Meteorol. Soc.* **142**, 1890–1903 (2016).
56. Wheelis, M. Biological warfare at the 1346 siege of Caffa. *Emerg. Infect. Dis.* **8**, 911–975 (2002).
57. Saiko, T. A. & Zonn, I. S. Irrigation expansion and dynamics of desertification in the Circum-Aral region of Central Asia. *Appl. Geogr.* **20**, 349–367 (2000).
58. Aldaya, M. M., Muñoz, G. & Hoekstra, A. Y. *Water Footprint of Cotton, Wheat and Rice Production in Central Asia* (UNESCO-IHE, 2010).
59. Karthe, D., Chalov, S. & Borcharadt, D. Water resources and their management in Central Asia in the early twenty first century: Status, challenges, and future prospects. *Environ. Earth Sci.* **73**, 487–499 (2015).
60. Shi, Y. et al. Recent and future climate change in northwest China. *Clim. Change* **80**, 379–393 (2007).
61. Harris, I. P. D. J., Jones, P. D., Osborn, T. J. & Lister, D. H. Updated high-resolution grids of monthly climatic observations—the CRU TS3.10 Dataset. *Int. J. Climatol.* **34**, 623–642 (2014).
62. Tucker, C. J. et al. An extended AVHRR 8-km NDVI data set compatible with MODIS and SPOT vegetation NDVI data. *Int. J. Remote Sens.* **26**, 4485–5598 (2005).
63. Wigley, T. M. L., Briffa, K. R. & Jones, P. D. On the average value of correlated time series, with applications in dendroclimatology and hydrometeorology. *J. Clim. Appl. Met.* **23**, 201–213 (1984).
64. Cook, E. R. & Kairiukstis, L. A. *Methods of Dendrochronology: Applications in the Environmental Sciences* (Kluwer Academic, Dordrecht, 1990).
65. Trouet, V. & Van Oldenborgh, G. J. KNMI Climate Explorer: A web-based research tool for high-resolution paleoclimatology. *Tree-Ring Res.* **69**, 3–13 (2013).
66. Haurwitz, M. W. & Brier, G. W. A critique of superposed epoch analysis method: Its application to solar-weather relations. *Mon. Weath. Rev.* **109**, 2074–2079 (1981).
67. Granger, C. W. J. & Newbold, P. *Forecasting Economic Time Series* 2nd edn (Academic Press, 1986).

ACKNOWLEDGEMENTS

This work was supported by the National Key R&D Program of China (2018YFA0606401), NSFC (U1803341 and 32061123008), and National Youth Talent Support Program. We thank Bakhtiyorov Zulfiyrov for his assistance in streamflow data collection.

AUTHOR CONTRIBUTIONS

F.C., Y.Y., S.Y., R.Z., H.S., Y.C., M.S., and H.Z. developed the original research design and collected and analyzed the historical documentary data. F.C., V.T., U.B., J.E., and F.H.C. wrote the article together and made the interpretations together. All authors reviewed the final manuscript.

COMPETING INTERESTS

The authors declare no competing interests.

ADDITIONAL INFORMATION

Supplementary information The online version contains supplementary material available at <https://doi.org/10.1038/s41612-022-00239-5>.

Correspondence and requests for materials should be addressed to Feng Chen or Fahu Chen.

Reprints and permission information is available at <http://www.nature.com/reprints>

Publisher's note Springer Nature remains neutral with regard to jurisdictional claims in published maps and institutional affiliations.



Open Access This article is licensed under a Creative Commons Attribution 4.0 International License, which permits use, sharing, adaptation, distribution and reproduction in any medium or format, as long as you give appropriate credit to the original author(s) and the source, provide a link to the Creative Commons license, and indicate if changes were made. The images or other third party material in this article are included in the article's Creative Commons license, unless indicated otherwise in a credit line to the material. If material is not included in the article's Creative Commons license and your intended use is not permitted by statutory regulation or exceeds the permitted use, you will need to obtain permission directly from the copyright holder. To view a copy of this license, visit <http://creativecommons.org/licenses/by/4.0/>.

© The Author(s) 2022